Exploring Effective Methods for Simulating Damaged Structures With Geometric Variation: Toward Intelligent Failure Detection

Daniel A. McAdams[1]
e-mail: dmcadams@umr.edu

David Comella

Department of Mechanical and Aerospace Engineering,
University of Missouri—Rolla,
Rolla, MO 65409-0050

Irem Y. Tumer
Complex Systems Design Group,
Intelligent Systems Division,
NASA Ames Research Center,
Moffett Field, CA 94035-1000
e-mail: itumer@mail.arc.nasa.gov

Inaccuracies in the modeling assumptions about the distributional characteristics of the monitored signatures have been shown to cause frequent false positives in vehicle monitoring systems for high-risk aerospace applications. To enable the development of robust fault detection methods, this work explores the deterministic as well as variational characteristics of failure signatures. Specifically, we explore the combined impact of crack damage and manufacturing variation on the vibrational characteristics of beams. The transverse vibration and associated eigenfrequencies of the beams are considered. Two different approaches are used to model beam vibrations with and without crack damage. The first approach uses a finite difference approach to enable the inclusion of both cracks and manufacturing variation. The crack model used with both approaches is based on a localized decrease in the Young's modulus. The second approach uses Myklestad's method to evaluate the effects of cracks and manufacturing variation. Using both beam models, Monte Carlo simulations are used to explore the impacts of manufacturing variation on damaged and undamaged beams. Derivations are presented for both models. Conclusions are presented on the choice of modeling techniques to define crack damage, and its impact on the monitored signal, followed by conclusions about the distributional characteristics of the monitored signatures when exposed to random manufacturing variations. [DOI: 10.1115/1.2188535]

Introduction

Background and Motivation. Effective failure detection requires a good understanding of the characteristics of the monitored data and a good sample of failure data. In the absence of a statistically significant sample of failure data, vehicle health monitoring systems for high-risk aerospace applications have to rely on anomaly detection algorithms that work around this problem. Prior work has shown that such algorithms work poorly for engineered systems operating in a highly variable environment. For anomaly detection algorithms to work effectively, a more comprehensive framework must be established to represent known sources of design, manufacturing, operational, and random variation. In the case of anomaly detection, it is necessary to understand the probabilistic footprint of all these combined effects on the signals being measured.

In the actual operating environment, aerospace systems exhibit significant variability [1–3]. Furthermore, variations introduced during design, manufacturing, and assembly significantly influence the final response characteristics of such systems [4,2]. Ongoing research at NASA Ames Research Center and at the University of Missouri—Rolla explores an empirical and simulation-based approach to help develop deterministic and probabilistic models of healthy and faulty data.

Previous work has been published which describes the attempt to capture the influence of design variations for dynamic systems using probabilistic models [5], as well as to reduce the effects of operational variations due to maneuvering on decisions about the vehicle's health [1]. Current efforts focus on modeling rare failure signatures to determine their distributional characteristics using both empirical and simulation-based data.

More specifically, health monitoring of gas turbine engines is of great interest due to the use of the engines as the source of primary propulsion and power in many aerospace and military applications. The unexpected failure of a gas turbine can stop missions and in the worst case result in the death of crew members. Health monitoring is an integral part of many maintenance plans; accurate and reliable health monitoring can result in significant cost savings.

As a result, this paper is building a knowledge base for the operational detection of cracked turbine blades in zero allowable fault systems. A crack in a blade rotating at high speed can devastate an engine beyond repair. An extensive postfracture failure analysis of a wind tunnel compressor blade was made by Hampton and Nelson [6] and reveals much about crack initiation and growth but this is far too late for many applications. Ganesan et al. [7] use a finite element method to study the dynamic response of high speed rotors with variation in elastic modulus and mass density. Turbine blades have complex geometries and are subject to complex excitation signals. With a long term goal to completely understand the vibrational response of healthy and damaged turbine blades subject to different excitations, we begin with the simpler problem of understanding the impact of design and manufacturing variations on healthy and damaged simple beams. As basic knowledge is developed, future work will explore the more complex turbine blade problem.

Paper Focus. In the first publication on the results of this work, the authors presented a feasibility study on the use of probabilistic methods (e.g., Monte Carlo simulation) using a simple example in design, and compared these methods to more traditional variation analysis techniques [5]. A case study was presented, focusing on

[1]Author to whom correspondence should be addressed.

Contributed by the Applied Mechanics Division of ASME for publication in the JOURNAL OF APPLIED MECHANICS. Manuscript received September 9, 2004; final manuscript received January 25, 2006. Review conducted by S. Govindjee. Discussion on the paper should be addressed to the Editor, Prof. Robert M. McMeeking, Journal of Applied Mechanics, Department of Mechanical and Environmental Engineering, University of California—Santa Barbara, Santa Barbara, CA 93106-5070, and will be accepted until four months after final publication of the paper itself in the ASME JOURNAL OF APPLIED MECHANICS.

the analysis of a lumped parameter dynamic model for a complex cam-follower, followed by an analysis of vibration data obtained from such a model. The Monte Carlo simulation technique was used to vary a subset of the design parameters. The effect on the vibration response was explored to determine whether probabilistic methods can be used to model the inherent variations observed in the dynamic response of complex systems [5]. Manufacturing process capability variations on as little as one of the modeling elements (e.g., the spring constant) were shown to cause significant variations in the acceleration signature of the cam-follower system.

A next set of publications addressed the question of whether these variations, caused by variations in the manufacturing process, would have an impact on the monitored signature when combined with a failure signature. A key effort required was the modeling of cracks in conjunction with variability. A modal analysis approach was presented in that work to explore the effect of variability and cracks together [8]. The results of the previous work indicated that the type of variation that can occur from standard manufacturing processes can cause complications in identifying damaged beams. Though the comparison of a damaged beam to an undamaged beam still results in the same trend (the eigenfrequencies of the damaged beam decrease as compared to the undamaged beam), the geometric variations result in a variation in eigenfrequencies on a scale similar to that resulting from damage.

To thoroughly simulate turbine blades, variations in material properties need to be included as well as variations in geometry. In addition, realistic turbine blade geometries need to be simulated as opposed to simple prismatic beams. Performing Monte Carlo simulations on more complex geometries with more sources of variation will be computationally expensive. Thus, determining an effective method for calculating the eigenfrequencies of damaged beams is important. In a previous effort, we discovered that using a direct modal approach had difficulty in calculating high-order eigenfrequencies [8]. In this paper, damage simulation is explored further by using two different modeling approaches to generate the failure signatures, and exploring their variational characteristics when combined with inherent variations in the system and/or its components. Specifically, models are derived to study the combined impact of crack damage and manufacturing variation on the vibrational characteristics of simple beams. The transverse vibration and associated eigenfrequencies of the beams are considered as the candidate monitoring signature.

Specifically, we are interested in methods that are computationally efficient and allow the inclusion of damage in the model formulation. The first approach uses a finite difference approach, initially presented in [8], to enable the inclusion of both cracks and manufacturing variation to be considered. The crack model used with both approaches is based on a localized decrease in Young's modulus. The second approach uses Myklestad's method. This method uses a lumped model of the beam to create a frequency equation which can then be solved to find the natural frequencies. Using both beam models, Monte Carlo simulations are used to explore the impact of manufacturing variation on damaged and undamaged beams.

Finite element method (FEM) approaches, such as cohesive zone finite element modeling, are not explored in this article. Finite element methods are perhaps the most versitile and effective approach to the analysis of dynamic structures. However, when applied to structures with uncertain properties, including geometry and material properties, the FEM faces some difficulties. To perform a Monte Carlo simulation each sample requires the generation of a different geometric structure with spatially random properties. After generating the structure, it needs to be decomposed or meshed, then solved and relevant information recorded. In many cases, meshing requires almost as much computation time as the solution. If 10,000 samples are needed to generate a sufficiently accurate simulation, the computational time becomes large.

In the following sections, detailed derivations are presented for both models, followed by their application to an example problem to determine the distributional characteristics. Conclusions are presented on the choice of modeling techniques to define crack damage, and its impact on the monitored signal, followed by conclusions about the distributional characteristics of the monitored signatures when exposed to random manufacturing variations.

Fault Detection and Health Monitoring Overview. The general problem of fault detection is reviewed by Lefas et al. [9]. Fault detection is conducted by checking that measured or estimated parameters are within set tolerances. Models are needed to relate directly measurable parameters to physical problems within the device. For instance, if the natural frequency of a beam can be measured, a model can be used to determine whether the beam is cracked. Using the model, the tolerance for the natural frequency can be set such that, if the natural frequency is outside the tolerance, confidence is high that a crack is present.

The final design of a health monitoring system for any turbomachinery is influenced by the maintenance philosophy which will be employed for the machines lifetime and the specific needs of the application. Four maintenance philosophies are reviewed by Pusey and Roemer [10]. The design of a health monitoring system requires the careful study of potential failure modes, their effects, and criticality of those effects. Banks et al. [11] review this process for the U.S. Marine Corps Advanced Amphibious Assault Vehicle (AAAV). Functional models and good system response models are needed to determine where a particular failure mode's symptoms would occur and how it could be measured [12,13]. Set points for alarms and automated responses can be established for the measured parameters. The costs and benefits must then be evaluated for the particular needs of an application. The trade off between false alarm rate and missed detection rate is one of the most difficult problems that must be balanced [14].

With respect to the current focus on turbine blades, the most commonly measured parameters for gas turbines are vibration, lubrication oil quality, and performance. Performance is calculated from the measured parameters of temperature, pressure, and flow rate [15]. Lifson et al. [16] analyze the practices, benefits, and limitations of several types of vibration monitoring systems used with industrial gas turbines.

This paper is building a knowledge base for the operational detection of cracked turbine blades in zero allowable fault systems. Blading problems are responsible for 42% of failures in gas turbines [17]. A crack in a blade rotating at high speed can devastate an engine beyond repair. Case studies have shown that common existing vibration monitoring systems on operating engines cannot detect a fatigue crack until a critical problem occurs [18]. Several methods of measuring the blade vibration have been reviewed by Al-Bedoor [19], including strain gauges, laser Doppler, lateral vibration, pressure fluctuations, torsional vibration, and piezoelectric materials. Most of these methods are still under investigation and are not intended for use on production engines. An extensive postfracture failure analysis of a wind tunnel compressor blade was made by Hampton and Nelson [6] and reveals much about crack initiation and growth but this is far too late for many applications. Ganesan et al. [7] use a finite element method to study the dynamic response of high speed rotors with variation in elastic modulus and mass density.

Turbine blades have complex geometries and are subject to complex excitation signals. With a long term goal to completely understand the vibrational response of healthy and damaged turbine blades subject to different excitations, we begin with the simpler problem of understanding the impact of manufacturing variations on healthy and damaged simple beams. As basic knowledge is developed and effective solution methods established, future work will explore the more complex turbine blade problem.

Modeling Vibration in Damaged Beams

A critical and observable impact of fractures on beam vibrational response is the difference in the eigenfrequencies for the damaged and undamaged beams. Most theoretical models of cracked beams begin with a Euler-Bernoulli beam and develop special considerations to model crack damage. Here, the Euler-Bernoulli beam is developed with considerations for manufacturing variation. Crack models are added to the resultant model to explore the impacts of both manufacturing variation and structural damage.

In the following sections, two different approaches are explored to model crack damage in simple beams. The derivations of the models are presented for each, followed by simulation results to explore the distributional characteristics of the vibrational response of cracked and uncracked beams when combined with manufacturing variations.

Damaged Models and Related Work. A large effort has been made to explore the vibrational characteristics of damaged beams. Doebling et al. [20] present a review of vibration-based damage identification methods. Damage identification methods can be classified as linear and nonlinear. Linear methods can be divided into model- and non-model-based methods. They can also be classified by the four levels of information they can provide:

Level 1: Determination that damage is present
Level 2: Level 1 plus the location of the damage
Level 3: Level 2 plus quantification of the severity of the damage
Level 4: Level 3 plus a prediction of the remaining life of the structure

There are three common types of crack models [21]; local stiffness reduction, discrete spring models, and complex models in two or three dimensions. Hu and Liang [22] use an integrated approach of a massless spring and a continuum damage concept to develop a crack detection technique. Gudmundson [23] developed models that enable the simulation of natural frequency changes of structures due to cracks and other geometrical changes. In Gudmundson [23] the models are benchmarked against finite element analysis and experimental results from Wetland [24]. Chondros et al. [25] developed a continuous vibration model for the lateral vibration of a cracked Euler-Bernoulli beam with open edge cracks. Chondros et al. have also explored a crack model for transverse, longitudinal, and other vibrations as well as beams with different end conditions [26–28]. Mengcheng [29] and Yokoyama [30] used a theoretical line-spring model and Euler-Bernoulli beam theory to approximate the response of cracked beam vibrations. Maiti [31] developed theoretical models for the vibration characteristics of cracked beams with a linearly variable cross section (wedge shaped beams). Zheng and Fan [32] developed a method to calculate the natural frequency of beams with an arbitrary number of cracks and a nonuniform cross section using a modified Fourier series. Using experimental methods, Ju et al. [33] diagnosed the fracture damage of structures using modal frequency methods. Kuang and Huang [34] tackled the problem of a blade crack on a rotating disk with many shrouded blades.

Most works with cracks use a linear open crack model where the opposing crack faces do not come in contact at any point during the vibration. There has been some recent work with nonlinear breathing or closing crack models [35–37]; these all indicate that the closing reduces the change in natural frequency reduction compared to the open crack models, making the practical problem of damage detection more difficult.

Despite the effort expended in developing models that can be used to simulate the vibrational characteristics of fractured beams, each of the models assumes a beam with ideal geometry and material properties. Little work has been done to determine the combined effects of manufacturing variation and fractures on vibrational characteristics of structures. Two such such models are developed in this article and are presented next. The fault detection models developed will provide level 1 information and use a stiffness reduction method to model damage.

A Finite Difference Approach. On approach to determining the vibration characteristics of a cracked beam with manufacturing variation is developed here. This approach uses a finite difference method to produce the complete spatial and time solution to the beam. To produce the specific frequency information needed to identify a crack, a fast Fourier transform (FFT) is used to extract frequency information from the complete solution. To model a crack, a local reduction in material stiffness is used to model the crack [38].

Problem Formulation. The derivation of the model begins with the Euler-Bernoulli beam equation:

$$\rho A\frac{\partial^2 w}{\partial t^2}+\frac{\partial^2}{\partial x^2}\left(EI\frac{\partial^2 w}{\partial x^2}\right)=f(x,t). \tag{1}$$

In the development of the finite difference equations in this section, the products ρA and EI will be kept together as a single term. Also, the explicit functional dependency of w on space and time is not shown to simplify notation. To allow geometric variation to enter the model, also, ρA and EI have spatial dependency. We are interested in the free response as only frequency information is needed, thus $f(x,t)=0$. Given this construction, the multiplication rule can be applied to give

$$\rho A\frac{\partial^2 w}{\partial t^2}+\frac{\partial^2 EI}{\partial x^2}\frac{\partial^2 w}{\partial x^2}+EI\frac{\partial^4 w}{\partial x^4}=0. \tag{2}$$

Equation (2) is a model of beam vibration that allows geometric variation to be included in the simulation. For the case presented here, a pinned-pinned beam will be simulated. The boundary conditions for the simply supported (pinned-pinned) case for the left end are that the deflection is zero,

$$w|_{x=0}=0, \tag{3}$$

and that the moment is zero,

$$EI\frac{\partial^2 w}{\partial x^2}\bigg|_{x=0}=0. \tag{4}$$

Similarly, for the right end the boundary conditions are that the deflection is zero,

$$w|_{x=L}=0 \tag{5}$$

and the moment is zero,

$$EI\frac{\partial^2 w}{\partial x^2}\bigg|_{x=L}=0. \tag{6}$$

The frequency behavior of damaged and undamaged beams will be extracted by applying an FFT to the complete solution of the finite difference model. To produce motion, initial conditions must be applied. The beam will be bent to an initial shape and then allowed to vibrate from rest. This results in the following initial conditions of

$$w|_{t=0}=w_0 \tag{7}$$

and

$$\frac{\partial w}{\partial t}\bigg|_{t=0}=0 \tag{8}$$

where w_0 is the initial beam shape. The problem is now fully formulated. We apply finite difference techniques in the next section.

Application of Finite Difference Techniques. To formulate algorithms for a computer program to solve, approximations for

the fourth- and second-order terms in Eq. (2) must be substituted. The second-order accurate approximation for the fourth-order term from Lapidus [39] is

$$\frac{\partial^4 w}{\partial x^4} = \frac{w_{i+2,j} - 4w_{i+1,j} + 6w_{i,j} - 4w_{i+1,j} + w_{i-2,j}}{(\Delta x)^4} \tag{9}$$

where i and j are integers representing the spatial step and the time step, respectively. The second-order accurate approximation for the second derivative of deflection with respect to x is

$$\frac{\partial^2 w}{\partial x^2} = \frac{w_{i+1,j} - 2w_{i,j} + w_{i-1,j}}{(\Delta x)^2} \tag{10}$$

Similar approximations are used for the second derivative of deflection with respect to time and the second derivative of EI with respect to x. The result is

$$\frac{\partial^2 w}{\partial t^2} = \frac{w_{i,j+1} - 2w_{i,j} + w_{i,j-1}}{(\Delta t)^2} \tag{11}$$

and

$$\frac{\partial^2 EI}{\partial x^2} = \frac{EI_{i+1} - 2EI_i + EI_{i-1}}{(\Delta x)^2}. \tag{12}$$

Substituting Eqs. (10)–(12) into Eq. (2) yields

$$\rho A_i \frac{(w_{i,j+1} - 2w_{i,j} + w_{i,j-1})}{(\Delta t)^2} + \left(\frac{EI_{i+1} - 2EI_i + EI_{i-1}}{(\Delta x)^2}\right) \times \left(\frac{w_{i+1,j} - 2w_{i,j} + w_{i-1,j}}{(\Delta x)^2}\right) + EI_i\left(\frac{w_{i+2,j} - 4w_{i+1,j} + 6w_{i,j} - 4w_{i-1,j} + w_{i-2,j}}{(\Delta x)^4}\right) = 0. \tag{13}$$

Solving for the $w_{i,j+1}$ term gives

$$w_{i,j+1} = 2w_{i,j} - w_{i,j-1} - \frac{(\Delta t)^2}{\rho A_i (\Delta x)^4}[(EI_{i+1} - 2EI_i + EI_{i-1})(w_{i+1,j} - 2w_{i,j} + w_{i-1,j}) + EI_i(w_{i+2,j} - 4w_{i+1,j} + 6w_{i,j} - 4w_{i-1,j} + w_{i-2,j})]. \tag{14}$$

Equation (14) can be used to calculate the deflection at a point on the beam at a time step, given knowledge of the deflection at that point at the two previous time steps, as well as knowledge of the deflection two spatial time steps to the left and to the right at the previous time step. This is an explicit finite difference form.

In addition to the general formulation of Eq. (14), finite difference expressions are needed for the boundary conditions and time and spatial steps where the two previous time steps are not known and the spatial steps are at the physical ends of the beam. Using a Taylor series expansion, the deflection at the first time step can be represented by

$$w_{i,1} = w_{i,0} + \Delta t \left.\frac{\partial w}{\partial t}\right|_{i,0} + (\Delta t)^2 \frac{1}{2} \left.\frac{\partial^2 w}{\partial t^2}\right|_{i,0}. \tag{15}$$

The first two terms on the right-hand side of Eq. (15) are known from the initial conditions, Eqs. (7) and (8). Substituting the initial conditions and solving for the second derivative with respect to time gives

$$\left.\frac{\partial^2 w}{\partial t^2}\right|_{i,0} = \frac{2(w_{i,j} - w_{i,0})}{(\Delta t)^2}. \tag{16}$$

Substituting Eqs. (16), instead of (11), along with Eqs. (9), (10), and (12) into Eq. (2) and solving for the deflection at the first time step gives

$$w_{i,1} = w_{i,0} - \frac{1}{2}\frac{(\Delta t)^2}{\rho A_i (\Delta x)^4}[(EI_{i+1} - 2EI_1 + EI_{i-1})(w_{i+1,0} - 2w_{i,0} + w_{i,0}) + EI_i(w_{i+2,0} - 4w_{i+1,0} + 6w_{i,0} - 4w_{i-1,0} + w_{i-2,0})]. \tag{17}$$

Equation (17) gives the deflection of the first time step for any point on the beam except the first and second points from the left or right where the terms $i+2$, $i+1$, $i-1$, and $i-2$ could have no meaning as those points do not exist on the beam. The boundary conditions must be used to give information about those points.

From the deflection boundary conditions (3) and (5), the deflection for the left and right ends of the beam is zero for all time steps

$$w_{1,j} = 0 \tag{18}$$

and

$$w_{n,j} = 0 \tag{19}$$

where $w_{n,j}$ represents the right end ($x=L$) and $w_{1,j}$ represents the left end ($x=0$).

Next, an expression for the second point from the left and right must be found from the other two boundary conditions (4) and (6). Writing Eq. (10) for the end points (1 and n) and using the boundary conditions to set the second derivative equal to zero yields

$$EI_1\left(\frac{w_{0,j} - 2w_{1,j} + w_{2,j}}{(\Delta x)^2}\right) = 0 \tag{20}$$

and

$$EI_n\left(\frac{w_{I+1,j} + 2w_{I,j} - w_{I-1,j}}{(\Delta x)^2}\right) = 0. \tag{21}$$

Substituting the values from Eqs. (18) and (19) into those above gives

$$w_{0,j} = -w_{2,j} \tag{22}$$

and

$$w_{n+1,j} = -w_{n-1,j}. \tag{23}$$

Writing Eq. (17) for the points 2 and $n-1$ and substituting into Eq. (18), (19), (22), and (23) results in expressions for these second points at the first time step. These expressions are

$$w_{2,1} = w_{2,0} - \frac{1}{2}\frac{(\Delta t)^2}{\rho A_2 (\Delta x)^4}[EI_2(w_{4,0} - 4w_{3,0} + 5w_{2,0}) + (EI_3 - 2EI_2 + EI_1)(w_{3,0} - 2w_{2,0})] \tag{24}$$

and

$$w_{n-1,1} = w_{n-1,0} - \frac{1}{2}\frac{(\Delta t)^2}{\rho A_2 (\Delta x)^4}[(EI_n - 2EI_{n-1} + EI_{n-2})(-2w_{n-1,0} + w_{n-2,0}) + EI_{n-1}(5w_{n-1,0} - 4w_{n-2,0} + w_{n-3,0})]. \tag{25}$$

Also, writing Eq. (14) about the same points as above but for any time step $j+1$ yields

$$w_{2,j+1} = 2w_{2,j} - w_{2,j-1} + \frac{(\Delta t)^2}{\rho A_2 (\Delta x)^4}[(EI_3 - 2EI_2 + EI_1)(w_{3,j} - 2w_{2,j}) + EI_2(w_{4,j} - 4w_{3,j} + 5w_{2,j})] \tag{26}$$

and

$$w_{n-1,j+1} = 2w_{n-1,j} - w_{n-1,j-1} + \frac{(\Delta t)^2}{\rho A_{n-1} (\Delta x)^4}[(EI_n - 2EI_{n-1} + EI_{n-2}) \times (-2w_{n-1,j} + w_{n-2,j}) + EI_{n-1}(5w_{n-1,j} - 4w_{n-2,j} + w_{n-3,j})]. \tag{27}$$

Equations (7), (17), (24), and (25) are used in a program to give a complete data set for the initial deflection of the beam and the

Table 1 Properties of the simulated beam.

Property	Value
Length	1 m
Nominal base	10 cm
Nominal base	10 cm
Nominal height	10 cm
E_0	93750 Pa
Density	1 kg/m^3
Crack depth	10 mm
Crack location	Midpoint

deflection of the first time step. Equations (26) and (27) are then calculated for a time step; Eq. (14) is then calculated for each internal point on the beam.

Since this is an explicit formulation, the choice of step sizes must meet the following stability criterion [40]:

$$2\sqrt{\frac{EI}{\rho A}}\frac{(\Delta t)}{(\Delta x)^2} \leq 1. \tag{28}$$

Parameter Variation and Crack Modeling. Using the finite difference technique developed above, solutions to Euler-Bernoulli beams with variation in the material properties and geometry can be found. This section will consider how the variation due to manufacturing tolerances and cracks was modeled. The *McGraw-Hill Machining and Metal Working Handbook* [41] gives tolerances for many manufacturing techniques and for different parts. Rarely do these tolerances exceed 1% of the nominal dimension. We will use this variation as to approximate geometric variations in the beam simulations below.

This paper considers a beam with a square cross section. To model manufacturing variation, the base and height may differ at any point on the beam's length by ±1% from the nominal dimension. Using the standard practice [42], a tolerance is equal to three times the standard deviation of a normal distribution. To generate these differences a random number generator was used with the base diminsion as the mean and a standard deviation of one third of the tolerance. Then, the base and height were generated for each of the desired subdivisions of the length and then substituted into the formulas for I and A. When multiplied by modulus of elasticity and density, this results in data for the $EI(x)$ and $pA(x)$ functions, thus providing a randomly varying geometry for the beam.

As discussed above, there are numerous crack and damage models in the literature. Here, the influence of the crack was modeled using the damage mechanics approach by DiPasquale [43]. The damage parameter is defined as

$$d = \frac{A_d}{A_T} \tag{29}$$

where $A_d = b \times a$.

Using the damage parameter the stiffness degradation in the area near the crack can be calculated as

$$E = (1 - d)E_0. \tag{30}$$

This degraded E is substituted into the EI formula for the node corresponding to the crack location. This incorporates the influence of the crack into the varying properties of the beam.

Example. The finite difference equations and crack model developed above were used to simulate the vibrational behavior of a cracked beam. The specific properties of the beam are shown in Table 1. Results of the distribution of the first five natural frequencies are presented for both a healthy and damaged beam below.

Results. A time marching program was developed in MATLAB utilizing the equations presented above to solve the Euler-Bernoulli beam. Ten thousand Monte Carlo simulates were run for an uncracked beam with a randomly varying geometry. The first five natural frequencies were recovered using fast Fourier transforms for each iteration. However, in a final detailed simulation, more than 10,000 runs would be used to create more accurate models. In this article we are only comparing the two methods so 10,000 samples is deemed sufficient. The histograms for the uncracked beam are shown in Figs. 1–5.

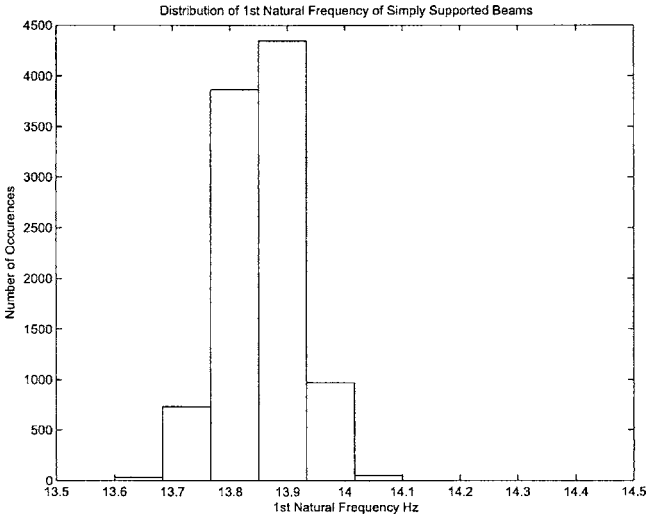

Fig. 1 Histogram for the first natural frequency of the uncracked beam (finite difference method)

The program was next modified to take into account the influence of a crack at the midpoint with a depth of 10 mm using the local stiffness degradation model presented above. Histograms for the first five natural frequencies are presented in Figs. 6–10.

Table 2 shows values for the mean and the standard deviation of the five recovered natural frequencies for the damaged and undamaged beams. The mean decreased as expected when the beam is cracked for the first, third, and fifth natural frequencies, but increased for the second and fourth natural frequencies. The increase in the second and fourth natural frequencies is inconsistent with both the experimental and theoretical literature on damaged beams. The increase in these natural frequencies represents an error in the simulation approach. The difference in standard deviation of the natural frequencies between cracked and uncracked

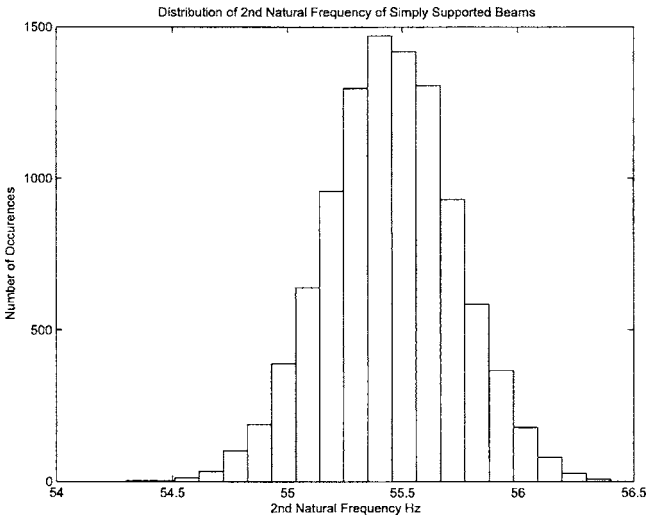

Fig. 2 Histogram for the second natural frequency of the uncracked beam (finite difference method)

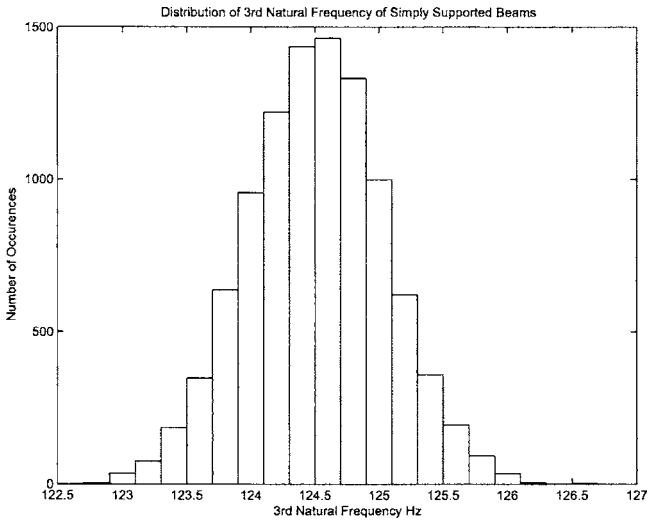

Fig. 3 Histogram for the third natural frequency of the uncracked beam (finite difference method)

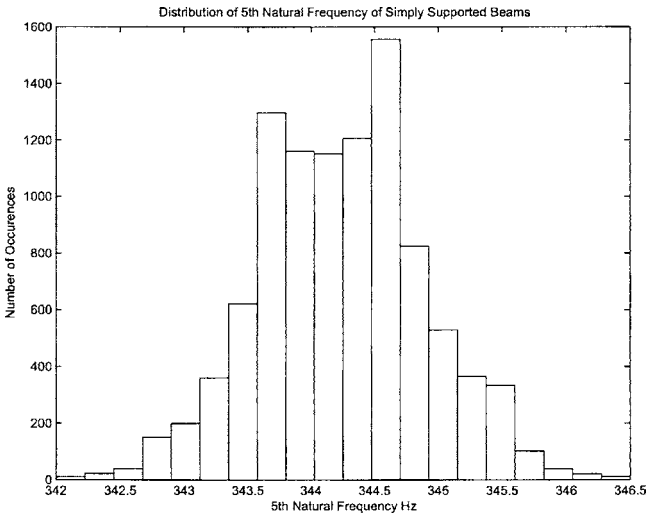

Fig. 5 Histogram for the fifth natural frequency of the uncracked beam (finite difference method)

cases was small for all frequencies except the first, which nearly doubled when cracked. The addition of manufacturing variations on the beam had little impact on the changes in natural frequency as compared to a beam of ideal geometry. Using this model, the conclusion would be that a shift in natural frequencies would be observable even under conditions of geometric variation. Also, the standard deviations are largely the same for uncracked and cracked beams.

The Myklestad Approach. A second approach to determining the vibration characteristics of a cracked beam with manufacturing variation is developed here. Myklestad [44] used a tabular method to perform the calculations. Here, we will use Myklestad's method with the transfer matrix approach developed by Thomson [45] and augmented by Pestel and Leckie [46]. In this approach a lumping method will create a model of the beam with point masses and stiffness fields. Transfer matrices will be written for each segment of the lumped beam. The matrices are then multiplied together to form an overall transfer matrix for the entire beam. Next, boundary conditions are then applied to produce the frequency equation. Finally, the roots of the frequency equation can then be solved to yield the natural frequencies.

Problem Formulation. Myklestad's method for bending vibration is effective for determining natural frequencies for a structure. This paper uses the notation and approach of Meirovitch [47]. First, a lumped model of the pinned-pinned beam must be constructed. The beam will be divided into ten equal increments with the lumped zero inertia masses placed in the center as shown in Fig. 11. Ten increments were used to satisfy the rule [48] that the number of concentrated masses should be at least twice the number of frequencies to be obtained.

The masses will be called "stations" and the space in between them will be referred to as "fields." Utilizing a free body diagram of a station, as shown in Fig. 12, and the equations of motion, a system of equations for the variables on the right can be written in matrix form

$$\begin{bmatrix} Y \\ \Psi \\ M \\ Q \end{bmatrix}_i^R = \begin{bmatrix} 1 & 0 & 0 & 0 \\ 0 & 1 & 0 & 0 \\ 0 & 0 & 1 & 0 \\ -\omega^2 m_i & 0 & 0 & 1 \end{bmatrix} \begin{bmatrix} Y \\ \Psi \\ M \\ Q \end{bmatrix}_i^L = T_{S,i} \begin{bmatrix} Y \\ \Psi \\ M \\ Q \end{bmatrix}_i^L . \quad (31)$$

Now an equation for the field will be developed from the free body diagram as shown in Fig. 13. Regarding the left end of the

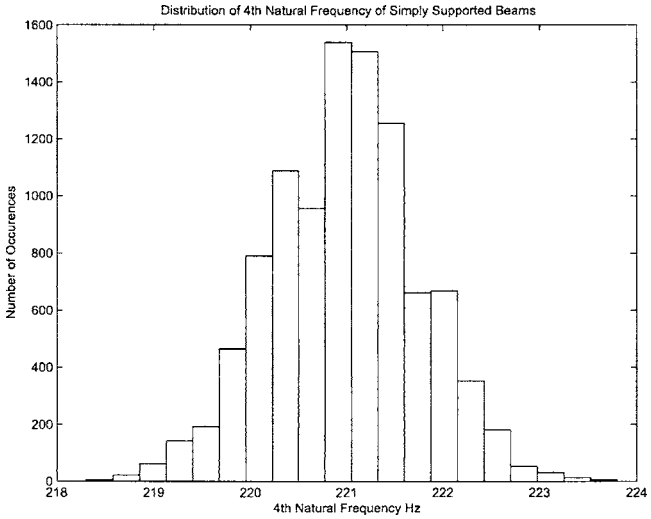

Fig. 4 Histogram for the fourth natural frequency of the uncracked beam (finite difference method)

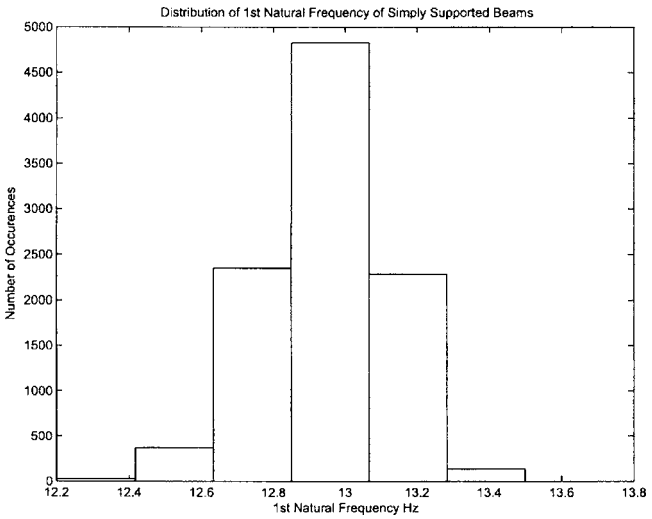

Fig. 6 Histogram for the first natural frequency of the cracked beam (finite difference method)

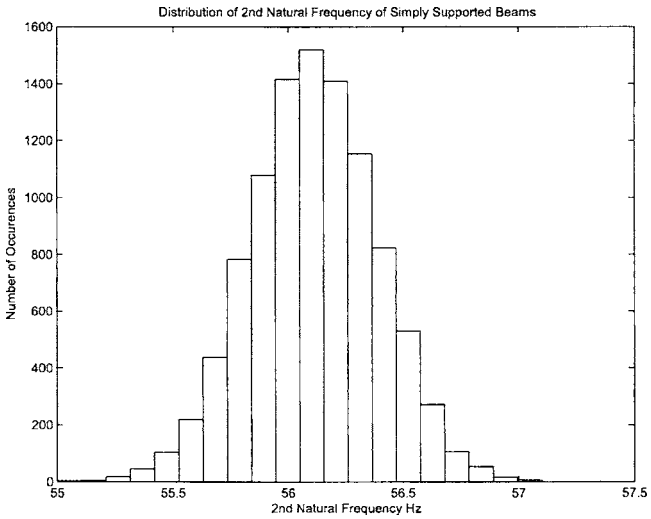

Fig. 7 Histogram for the second natural frequency of the cracked beam (finite difference method)

field as clamped, the equivalent spring equations for cantilevered beams can be introduced in the equations for deflection and angle. These relations coupled with equations of motion yield the following transfer matrix for the ith field.

$$\begin{bmatrix} Y \\ \Psi \\ M \\ Q \end{bmatrix}_{i+1}^{L} = \begin{bmatrix} 1 & \Delta x_i & (\Delta x_i)^2/2EI_i & -(\Delta x_i)^3/6EI_i \\ 0 & 1 & \Delta x/EI_i & -(\Delta x_i)^2/2EI_i \\ 0 & 0 & 1 & -\Delta x_i \\ 0 & 0 & 0 & 1 \end{bmatrix} \begin{bmatrix} Y \\ \Psi \\ M \\ Q \end{bmatrix}_{i}^{R} = T_{F,i} \begin{bmatrix} Y \\ \Psi \\ M \\ Q \end{bmatrix}_{i}^{R} . \quad (32)$$

Substituting Eq. (31) into Eq. (32) yields the transfer equation for the station vector of the left side of station $i+1$ to the station vector on the left side of station i

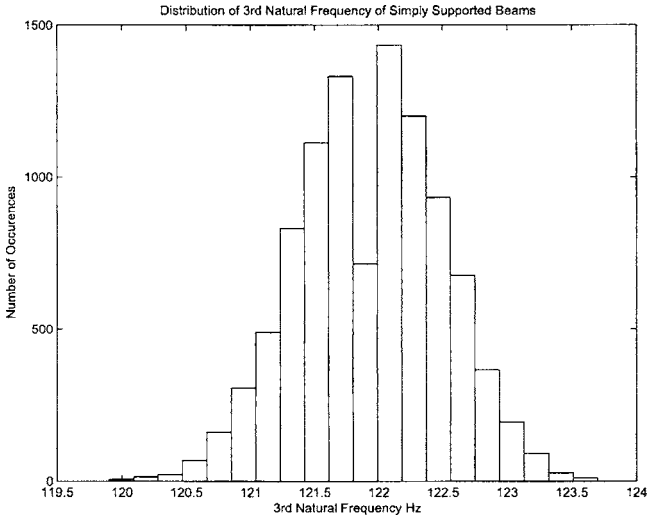

Fig. 8 Histogram for the third natural frequency of the cracked beam (finite difference method)

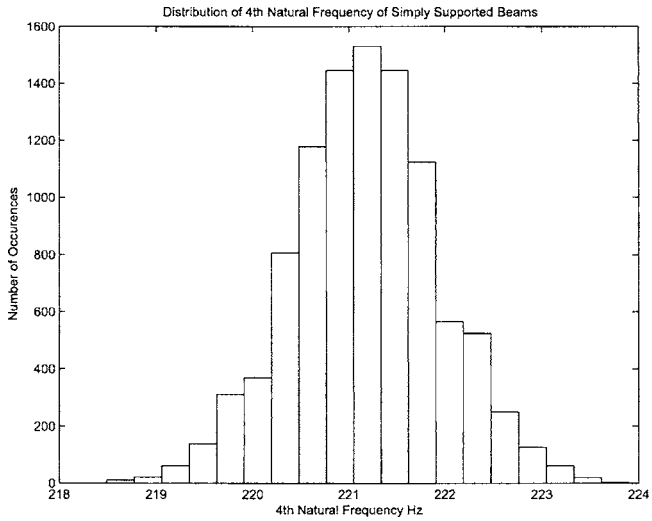

Fig. 9 Histogram for the fourth natural frequency of the cracked beam (finite difference method)

$$\begin{bmatrix} Y \\ \Psi \\ M \\ Q \end{bmatrix}_{i+1}^{L} = T_i \begin{bmatrix} Y \\ \Psi \\ M \\ Q \end{bmatrix}_{i}^{L} , \quad (33)$$

where T_i is the transfer matrix for the ith combination of station and field given by the product of the two matrixes

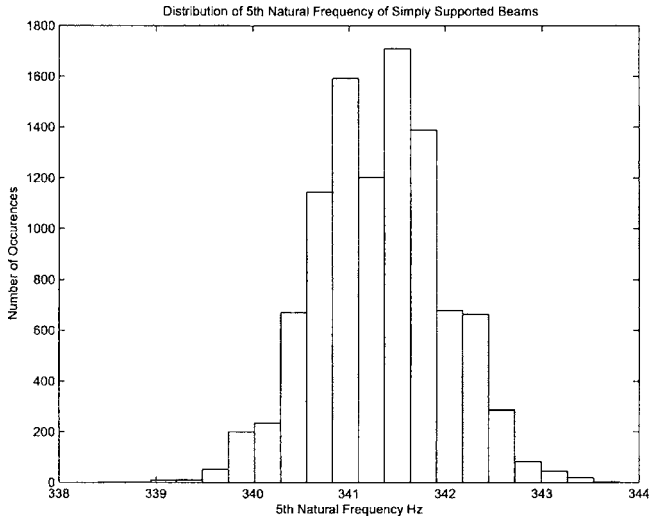

Fig. 10 Histogram for the fifth natural frequency of the cracked beam (finite difference method)

Table 2 The mean and standard deviation for the five natural frequencies (f_n) recovered

	Undamaged	Cracked
f_{n1} Mean	13.8505	12.9380
f_{n1} StDev	0.0799	0.1585
f_{n2} Mean	55.4427	56.109
f_{n2} StDev	0.2702	02638
f_{n3} Mean	124.5604	121.9362
f_{n3} StDev	0.5343	0.5561
f_{n4} Mean	220.9936	221.1734
f_{n4} StDev	0.7692	0.7672
f_{n5} Mean	344.2524	341.3335
f_{n5} StDev	0.6542	0.6590

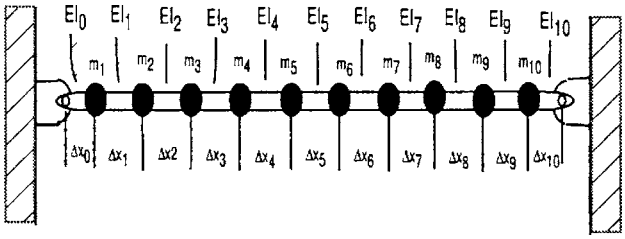

Fig. 11 Lumped model for a pinned-pinned beam

$$T_i = T_{F,i}T_{S,i} = \begin{bmatrix} 1+\omega^2 m_i(\Delta x_i)^3/6EI_i & \Delta x_i & (\Delta x_i)^2/2EI_i & -(\Delta x_i)^3/6EI_i \\ \omega^2 m_i(\Delta x_i)^2/2EI_i & 1 & \Delta x_i/EI_i & -(\Delta x_i)^2/EI_i \\ \omega^2 m_i \Delta x_i & 0 & 1 & -\Delta x_i \\ -\omega^2 m_i & 0 & 0 & 1 \end{bmatrix}. \tag{34}$$

Now the overall transfer matrix for the whole beam can be written by multiplying all of the individual transfer matrices together with the first field matrix

$$T = T_n T_{n-1} \cdots T_2 T_1 T_{F,0}. \tag{35}$$

The overall transfer matrix is a 4×4 matrix whose terms are functions of the eigenvalues, expressed in generic terms as

$$T = \begin{bmatrix} T_{1,1}(\omega^2) & T_{1,2}(\omega^2) & T_{1,3}(\omega^2) & T_{1,4}(\omega^2) \\ T_{2,1}(\omega^2) & T_{2,2}(\omega^2) & T_{2,3}(\omega^2) & T_{2,4}(\omega^2) \\ T_{3,1}(\omega^2) & T_{3,2}(\omega^2) & T_{3,3}(\omega^2) & T_{3,4}(\omega^2) \\ T_{4,1}(\omega^2) & T_{4,2}(\omega^2) & T_{4,3}(\omega^2) & T_{4,4}(\omega^2) \end{bmatrix}. \tag{36}$$

The relationship between the two pinned ends ($i=0$ and $i=11$) can now be expressed as

$$\begin{bmatrix} Y \\ \Psi \\ M \\ Q \end{bmatrix}_{n+1} = T \begin{bmatrix} Y \\ \Psi \\ M \\ Q \end{bmatrix}_0. \tag{37}$$

For the pinned-pinned case the deflection and bending moments are zero at the ends giving end conditions of

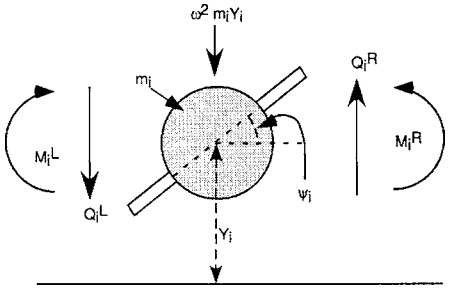

Fig. 12 Free-body diagram for station I

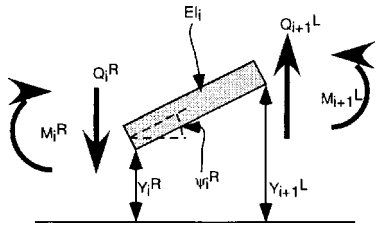

Fig. 13 Free-body diagram for station I

$$Y_0 = 0, \quad M_0 = 0, \quad Y_{n+1} = 0, \quad M_{n+1} = 0. \tag{38}$$

Substituting the values of Eq. (38) and the generic terms of Eq. (36) into Eq. (37) gives

$$0 = T_{1,2}(\omega^2)\Psi_0 + T_{1,4}(\omega^2)Q_0, \tag{39}$$

$$\Psi_{n+1} = T_{2,2}(\omega^2)\Psi_0 + T_{2,4}(\omega^2)Q_0, \tag{40}$$

$$0 = T_{3,2}(\omega^2)\Psi_0 + T_{3,4}(\omega^2)Q_0, \tag{41}$$

$$Q_{n+1} = T_{4,2}(\omega^2)\Psi_0 + T_{4,4}(\omega^2)Q_0. \tag{42}$$

The system of equations from Eqs. (39)–(41) have a nontrivial solution if

$$\det\begin{bmatrix} T_{1,2}(\omega^2) & T_{1,4}(\omega^2) \\ T_{3,2}(\omega^2) & T_{3,4}(\omega^2) \end{bmatrix} = T_{1,2}(\omega^2)T_{3,4}(\omega^2) - T_{1,4}(\omega^2)T_{3,2}(\omega^2) = 0. \tag{43}$$

Finding the roots of Eq. (43) gives the eigenvalues whose square roots are the natural frequencies or natural frequencies. In order to determine the roots, we have to generate sets of the lumped parameters m, EI, and a step size (Δx), then substitute that data into the equations above and find the roots of the frequency equation (43). The process of developing the variable parameters is described in the next section.

Parameter Variation and Crack Modeling. The reason for using Myklestad's method was to find solutions to Euler-Bernouilli beams with variation in the material properties and geometry. This section will consider how the variation due to manufacturing tolerance and cracks can be modeled and included in the Myklestad's formulation.

Again, we will use a ±1% tolerance on geometric variation. Also, the tolerance is considered equal to three times the standard deviation of a normally distributed parameter. Using the same beam as above, we consider a beam with a square cross section but the base and height may differ at any point on the beam's length. To generate these differences a random number generator was used with the base dimension as the average and a variance based on the 1% tolerance.

The base and hight were generated separately for a number of desired subdivisions of the length and then substituted into the formulas for I and A. When I is multiplied by the modulus of elasticity it produces the stiffness field parameter EI for that field. The value for A is multiplied by density and step size to give the value of the local lumped mass (m_i). Also, as used for the finite difference formulation, the influence of the crack was modeled using the same local stiffness degradation method as was used in the finite difference section.

Results. A program was developed in MATLAB to solve the same beam as presented in Table 1 in the finite difference section. Ten thousand Monte Carlo simulations were run for the uncracked beam with a randomly varying geometry. In a final detailed simulation, more than 10,000 runs would be used to create more accurate models. In this article we are only comparing the two methods so 10,000 samples is deemed sufficient. The first five natural frequencies were solved for each iteration. The histograms for the uncracked beam are shown in Figs. 14–18.

The program was next modified to take into account the influence of a crack at the midpoint with a depth of 10 mm using the local stiffness degradation model presented above. Histograms for the first five natural frequencies are presented in Figs. 19–23.

Table 3 shows values for the mean and the standard deviation of the first five natural frequencies for the damaged and undamaged beams. The mean decreased as expected when the beam is cracked for all natural frequencies. This result is consistent with both the experimental and theoretical literature on damaged and cracked beams. The standard deviation increased for the odd natural frequencies but decreased for the even ones. Again, the addition of

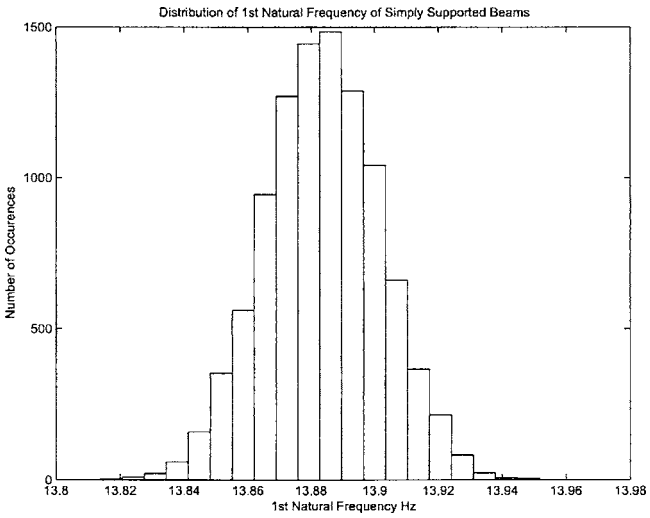

Fig. 14 Histogram for the first natural frequency of the uncracked beam (Myklestad's method)

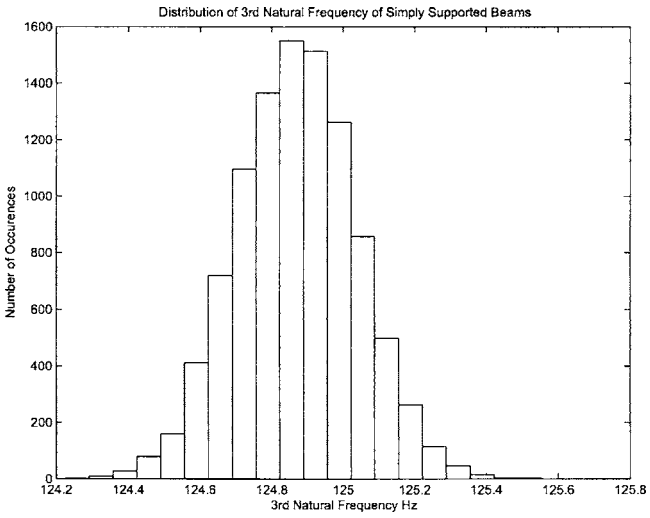

Fig. 16 Histogram for the third natural frequency of the uncracked beam (Myklestad's method)

manufacturing variations on the beam had little impact on the changes in natural frequency as compared to a beam of ideal geometry. Also, the standard deviations are largely the same for uncracked and cracked beams.

Discussion: Comparison of Modeling Approaches. To perform Monte Carlo simulations of a damaged turbine blade with the inclusion of variations in the model requires methods that run quickly and provide quantitative results consistent with the experimental and theoretical literature. Here the finite difference approach and Myklestad's method are compared with respect to their future applicability to realistic turbine blades.

Comparing the modeling approaches, both give largely the same results for the vibrational behavior of the beam. It does appear that the finite difference method introduces some numerical error with respect to the appropriate trends in natural frequency behavior. Myklestad's method can run much faster than the finite difference technique (more than 800 times faster). This is because the finite difference approach has to calculate the behavior of the beam for all points in space and a large enough sample length in time to recover the natural frequencies. Myklestad's method only requires solving the frequency equation for the number of natural frequencies desired.

Another advantage of Myklestad's method is its flexibility. The nominal properties of the beam analyzed in this paper were intentionally selected to have an unrealistically low modulus of elasticity. Common structural materials have modulus measured in GPa. To analyze beams with such high nominal modulus would require extremely small time step sizes to meet the stability criterion and the sampling frequency requirements. This would increase the already large computational time and memory requirements to prohibitive levels for the common personal computer.

The finite difference approach has the disadvantage that it does not directly supply frequency information. An FFT is used to extract the frequency information from the complete response. The frequency resolution of the recovered frequencies is dependent on the length of time the FFT samples. The larger the amount of time simulated, the better (i.e., smaller) the resolution. However, increasing the amount of data generated increases the demand on computer resources. Another problem with the recovery of frequency information by FFT is the leakage phenomena. Because the dimensions of the beam are randomly generated it is impossible to match the sampling period (i.e., record length) to the natural frequencies of the beam. This mismatch causes false natu-

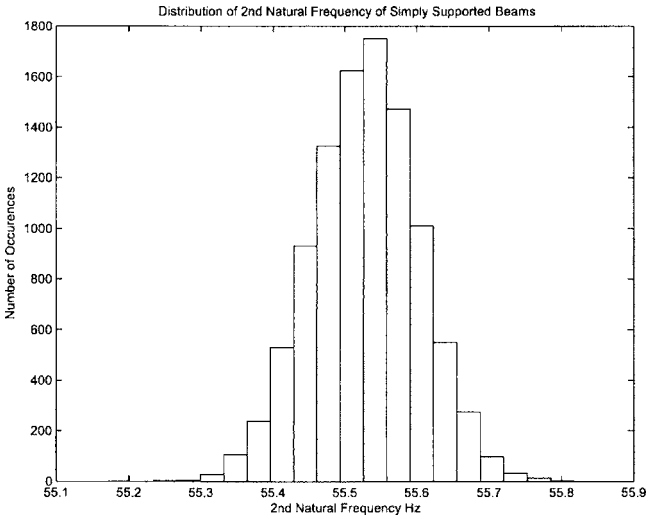

Fig. 15 Histogram for the second natural frequency of the uncracked beam (Myklestad's method)

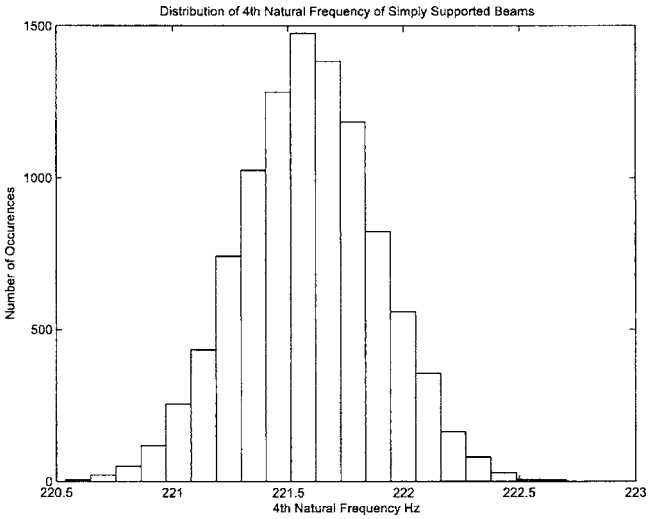

Fig. 17 Histogram for the fourth natural frequency of the uncracked beam (Myklestad's method)

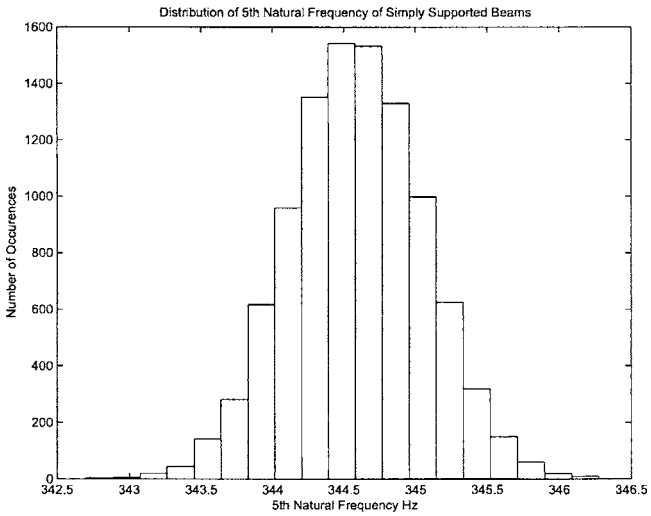

Fig. 18 Histogram for the fifth natural frequency of the uncracked beam (Myklestad's method)

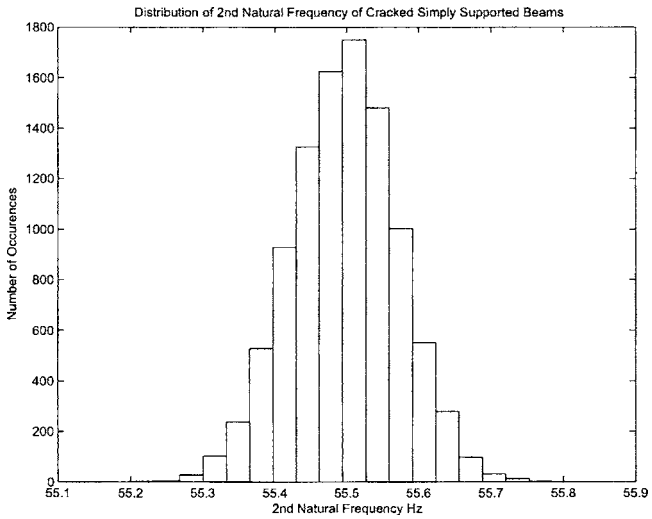

Fig. 20 Histogram for the second natural frequency of the cracked beam (Myklestad's method)

ral frequencies to be recorded near true natural frequencies. The false natural frequencies must be filtered out before meaningful interpretation of the data can be conducted. Myklestad's method has none of these problems as the natural frequencies are directly solved for.

Myklestad's method is superior to the finite difference method for the purposes of analyzing realistic structures with limited computing resources. This makes it the method of choice for simulating damaged structures. From both of these methods, we can conclude that geometric variation due to manufacturing tolerances alone is not likely to mask our ability to detect the presence of a crack that penetrates to 10% or more of the beam's depth by measuring the natural frequencies. The decrease in the natural frequencies in the damaged beams exceeds the standard deviation of the undamaged beams. Additional work to confirm this hypothesis will be discussed in the next section.

Summary and Future Work

In this article, the impact of manufacturing variations on the vibrational behavior of healthy and damaged pinned-pinned beams was explored. These modeling methods are being developed toward a long term goal of generating a complete understanding of realistic turbine blade behavior with respect to health monitoring. Specifically, we are interested in determining the way in which geometric and material variations interact with the vibrational behavior of the turbine blade and obfuscate fault detection.

Two solution methodologies are employed. The first uses a finite difference method to produce a complete solution to an undamaged and damaged beam. Fast Fourier transforms are used to extract frequency information from the complete response. The second develops a lumped beam model and uses transfer matrices to construct a frequency equation that can be solved to find the characteristics of the damaged and undamaged beam. Both solution methods gave similar results. The inclusion of manufacturing variation on a pinned-pinned beam of the nominal characteristics simulated here has minimal impact on changes in natural frequencies as compared to a significant crack.

Additional other methods in computational fracture mechanics still need to be explored, for example, the stochastic finite element method (SFEM). The SFEM has the advantage that it extends simply to structures of high geometric complexity. Also, developing efficient computational methods is facilitated by the wealth of existing numerical solution approaches. Also the SFEM integrates

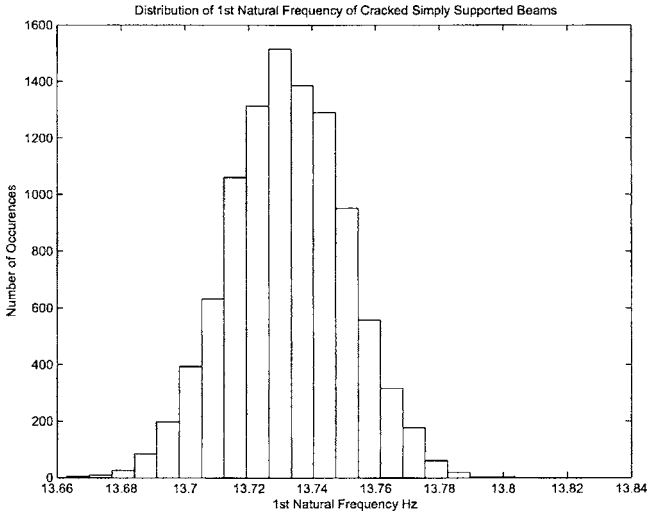

Fig. 19 Histogram for the first natural frequency of the cracked beam (Myklestad's method)

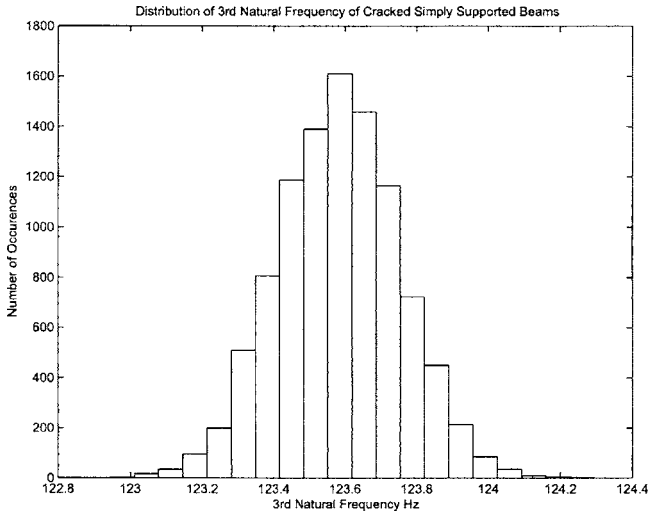

Fig. 21 Histogram for the third natural frequency of the cracked beam (Myklestad's method)

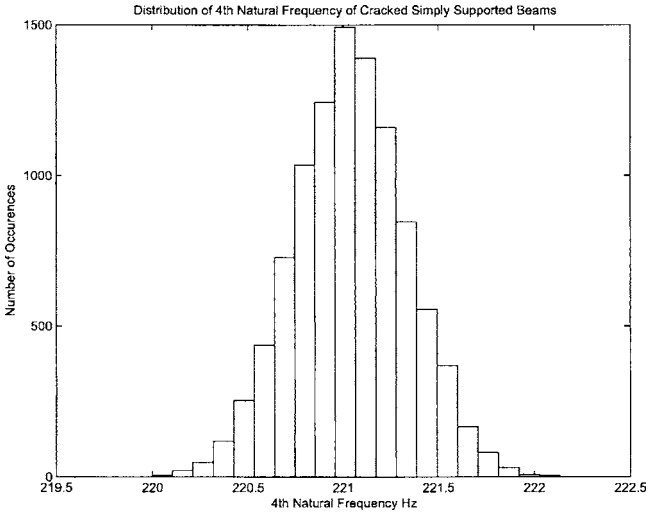

Fig. 22 Histogram for the fourth natural frequency of the cracked beam (Myklestad's method)

well with many of the crack models that are modeled using FEM techniques. One of the key advantages of the SFEM is that it does not require Monte Carlo simulation, thus it is computationally inexpensive compared to Monte Carlo based simulations. Also, multi-scale methods need to be explored.

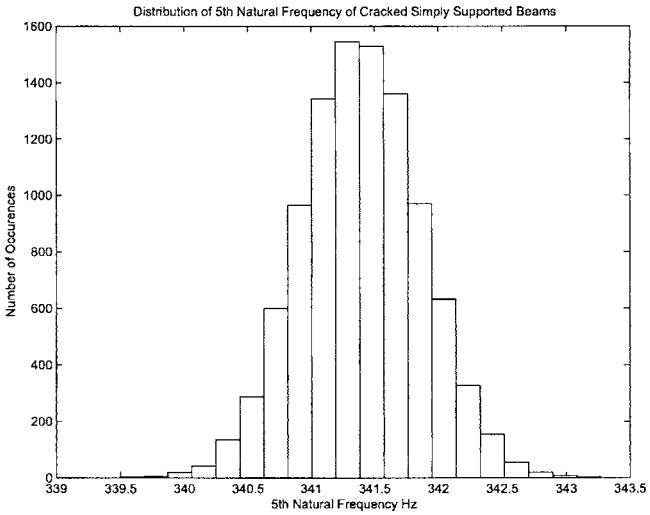

Fig. 23 Histogram for the fifth natural frequency of the cracked beam (Myklestad's method)

Table 3 The mean and standard deviation for the five natural frequencies (f_n)

	Undamaged	Cracked
f_{n1} Mean	13.8835	13.7324
f_{n1} StDev	0.0181	0.184
f_{n2} Mean	55.5284	55.49
f_{n2} StDev	0.0739	0.0738
f_{n3} Mean	124.8702	123.5825
f_{n3} StDev	0.1672	0.1694
f_{n4} Mean	221.5910	221.0384
f_{n4} StDev	0.2995	0.2968
f_{n5} Mean	344.5878	341.3925
f_{n5} StDev	0.4688	0.4710

To more realistically simulate actual turbine blades, critical future work includes developing models that allow the inclusion of variations in material properties such as density and Young's modulus. Additionally, more accurate representations of realistic turbine blade geometry need to be simulated. The current work has been limited to prismatic beams. The interaction between damaged and the more complex geometries of turbine blades needs to be explored.

Once the theoretical work has been developed to allow realistic turbine blades to be simulated, experimental validation is required. Experimental validation will begin with benchmarking theoretical models against simple prismatic structures and turbine blade geometries. Additionally, different crack models need to be explored and compared to determine which give the most accurate results when the models include damage.

Acknowledgment

This research was supported by NASA's Intelligent Data Understanding project of the Intelligent Systems/CICT program, and funded through a cooperative agreement NCC 2-5490.

Nomenclature

a = crack depth
b = width of beam
c = local compliance of the damaged beam
d = damage parameter
$f(x,t)$ = external force applied to a beam
h = height of a beam's cross section
i = integer multiplier for axial location
j = integer multiplier for time
n = denotes the left end of the beam
t = time
w = lateral deflection of the beam as a function of space and time
$w_0(x)$ = initial deflection of the beam
x = horizontal coordinate
A = cross-sectional area of the beam cross section
A_d = area of a beam's cross section affected by damage
A_t = total area of a beam's cross section
E = Young's modulus of elasticity
E_o = undamaged or ideal Young's modulus of elasticity
EI = flexural stiffness of a beam
I = area moment of inertia
L = length of beam
β = nondimensional horizontal crack location
λ = ratio of crack depth to beam height
ν = Poisson's ratio
ρ = density
I = area moment of inertia
ρA = mass per unit length of a beam
Δt = uniform time step size
Δx = uniform axial step size
Y = vertical position of a beam segment
Ψ = angle of a deflected beam
M = bending moment
Q = shearing force
T = transfer matrix
ω^2 = eigenvalue
m = mass of a beam segment

References

[1] Oza, N., Tumer, I., Tumer, K., and Huff, E., 2003, "Classification of Aircraft Maneuvers for Fault Detection," *Proceedings of the Multiple Classifier Systems (MCS) Workshop*.
[2] Tumer, I., and Huff, E., 2002, "On the Effects of Production and Maintenance

Variations on Machinery Performance," J. Qual. Maint. Eng., **8**(3), pp. 226–238.
[3] Tumer, I., and Huff, E., 2002, "Analysis of Triaxial Vibration Data for Health Monitoring of Helicopter Gearboxes," ASME J. Vibr. Acoust., **125**(1), pp. 120–128.
[4] Huff, E., Tumer, I., Barszcz, E., Dzwonczyk, M., and McNames, J., 2002, "Analysis of Maneuvering Effects on Transmission Vibrations in an AH-1 Cobra Helicopter," J. Am. Helicopter Soc., **47**(1), pp. 42–49.
[5] McAdams, D., and Tumer, I., 2002, "Towards Failure Modeling in Complex Dynamic Systems: Impact of Design and Manufacturing Variations," ASME Design for Manufacturing Conference, Vol. DETC2002/DFM-34161.
[6] Hampton, R., and Nelson, H. G., 1986, "Failure Analysis of a Large Wind Compressor Blade," ASTM Spec. Tech. Publ., **918**, pp. 153–180.
[7] Ganesan, R., Ramu, S., and Sankar, T., 1993, "Stochastic Finite Element Analysis for High Speed Rotors," ASME J. Vibr. Acoust., **115**(3), pp. 59–64.
[8] McAdams, D. A., Comella, D., and Tumer, I. Y., 2003, "Developing Variational Vibration Models of Damaged Beams: Toward Intelligent Failure Detection," *Proceedings ASME International Mechanical Engineering Congress and Expo*, No. IMECE 2003-42540, ASME, New York.
[9] A. Pouliezos, G. S., and Lefas, C., 1989, "Fault Detection Using Parameter Estimation," Qual. Reliab. Eng. Int, **5**, pp. 283–290.
[10] Pusey, H. C., and Roemer, M. J., 1999, "An Assessment of Turbomachinery Condition Monitoring and Failure Prognosis Technology," Shock Vib. Dig., **31**(5), pp. 365–371.
[11] Banks, J., Reichard, K., and Brought, M., 2002, "Development of the Asset Health Management System for the Marine Corps Advanced Amphibious Assult Vehicle," Proc. Society Mach. Failure Prevention Technol., **56**(2), pp. 277–286.
[12] Roemer, M. J., Kacprzynski, G. J., and Hess, A. J., 2002, "Health Management System Design: Development, Simulation and Cost/Benefit Optimization," *Proceedings of IEEE Conference*, Vol. 6, March, IEEE, Piscataway, NJ, pp. 3065–3072.
[13] Roemer, M. J., Kacprzynski, G. J., and Hess, A. J., 2001, "Extending FMECA-Health Management Design Optimization for Aerospace Applications," *Proceedings of IEEE Conference*, Vol. 6, March, IEEE, Piscataway, NJ, pp. 3105–3065.
[14] Ding, S. X., Frank, P. M., Ding, E., and Jeinsch, T., 2000, "Fault Detection System Design Base on a New Trade-off Strategy," *Proceedings of the 39th IEEE Conference on Decision and Control*, Vol. 4, December, IEEE, Piscataway, NJ, pp. 4144–4149.
[15] Phillips, J. N., Levine, P., and Tustain, S., 2000, "Performance Monitoring of Gas Turbine," *CO-MADE'2000 Proceedings of the 13th International Congress on Condition Monitoring and Diagnostic Engineering*, Houston, December 3–8, pp. 527–536.
[16] Lifson, A., Quentin, G., Smalley, A., and Knauf, C., 1989, "Assessment of Gas Turbine Vibration Monitoring," ASME J. Eng. Gas Turbines Power, **111**(2), pp. 257–263.
[17] Meher-Homji, C. B., and Gabriles, G., 1998, "Gas Turbine Blade Failure—Causes, Avoidance, and Troubleshooting," *Turbomachinery Symposium 1998: Proceedings of the Twenty-Seventh Turbomachinery Symposium*, Houston, September 20–24, pp. 129–179.
[18] Kumar, A., Kumar, V., and Hazara, U., 1996, "Effective Failure Analysis of Gas Turbine—A Need of Improved Monitoring System (A Case Study)," *COMADE'96 Proceedings of the Diagnostic Engineering Management Conference*, Sheffield, UK, June, pp. 905–915.
[19] Al-Bedoor, B. O., 2002, "Blade Vibration Measurement in Turbo-Machiner: Current Status," Shock Vib. Dig., **34**(6), pp. 455–461.
[20] Doebling, S. W., Farrar, C. R., and Prime, M. B., 1998, "A Summary Review of Vibration-Based Damage Identification Methods," Shock Vib. Dig., **30**(2), pp. 91–105.
[21] Friswell, M. I., and Penny, J. E. T., 2002, "Crack Modeling for Structural Health Monitoring," Struct. Health Monit., **1**(2), pp. 139–148.
[22] Hu, J., and Liang, Y., 1993, "An Integrated Approach to Detection of Cracks Using Vibration Characteristics," J. Franklin Inst., **330**(5), pp. 841–853.
[23] Gudmundon, P., 1982, "Eigenfrequency Changes of Structures Due to Cracks, Notches or Other Geometrical Changes," J. Mech. Phys. Solids, **30**(5), pp. 339–353.
[24] Wetland, D., 1972, "Aenderung der Biegeeigenfrequenzen einer idealisierten Schaufel durch Risse," Ph.D. thesis, University of Karlsruhe.
[25] Chondros, T. G., Dimarogonas, A. D., and Yao, J., 1998, "A Continuous Cracked Beam Vibration Theory," J. Sound Vib., **215**(1), pp. 17–34.
[26] Chondros, T. G., and Dimarogonas, A. D., 1998, "Vibration of a Cracked Cantilever Beam," Trans. ASME, J. Vib. Acoust., **120**(2), pp. 742–746.
[27] Chondros, T. G., Dimarogonas, A. D., and Yao, J., 1998, "Longitudinal Vibration of a Continuous Cracked Bar," Eng. Fract. Mech., **61**(5–6), pp. 593–606.
[28] Chondros, T. G., 2001, "The Continuous Crack Flexibility Model for Crack Identification," Fatigue Fract. Eng. Mater. Struct., **24**(10), pp. 643–650.
[29] Mengcheng, C., and Renji, T., 1997, "An Approximate Method of Response Analysis of Vibrations for Cracked Beams," Appl. Math. Mech., **18**(3), pp. 221–228.
[30] Yokoyama, T., and Chen, M.-C., 1998, "Vibration Analysis of Edge-Cracked Beams Using a Line-Spring Model," Eng. Fract. Mech., **59**(3), pp. 403–409.
[31] Chaudhari, T. D., and Maiti, S. K., 1999, "Modelling of Transverse Vibration of Beam of Linearly Variable Depth With Edge Crack," Eng. Fract. Mech., **63**(4), pp. 425–445.
[32] Zheng, D. Y., and Fan, S. C., 2001, "Natural Frequencies of a Non-Uniform Beam With Multiple Cracks Via Modified Fourier Series," J. Sound Vib., **242**(5), pp. 701–717.
[33] Ju, F. D., and Mimovich, M. E., 1988, "Experimental Diagnosis of Fracture Damage in Structures by the Modal Frequency Method," Trans. ASME, J. Vib. Acoust., **110**(4), pp. 456–463.
[34] Kuang, J. H., and Huang, B. W., 1999, "The Effect of Blade Crack on Mode Localization in Rotating Bladed Disks," J. Sound Vib., **227**(1), pp. 85–103.
[35] Chondross, T. G., Dimarogonas, A. D., and Yao, J., 2001, "Vibration of a Beam With a Breathing Crack," J. Sound Vib., **239**(1), pp. 57–67.
[36] Bovsunovsky, A. P., and Matveev, V. V., 2000, "Analytical Approach to the Determination of Dynamic Characteristics of a Beam With a Closing Crack," J. Sound Vib., **235**(3), pp. 415–434.
[37] Surace, N. P. C., and Ruotolo, R., 2000, "Evaluation of the Non-Linear Dynamic Response to Harmonic Exitation of a Beam With Several Breathing Cracks," J. Sound Vib., **235**(5), pp. 749–762.
[38] Kachanov, L., 1986, *Introduction to Continuum Damage Mechanics*, Martinus Nijhoff Publishers, Dordrecht, The Netherlands.
[39] Lapidus, L., and Pinder, G., 1982, *Numerical Solution of Partial Differential Equations in Science and Engineering*, John Wiley and Sons, New York.
[40] Bilbao, S., 2002, "Wave and Scattering Methods for the Numerical Integration of Partial Differential Equations," Ph.D. thesis, Stanford University.
[41] Walsh, R., 1999, *McGraw-Hill Machining and Metal Working Handbook*, McGraw-Hill, New York.
[42] Bowker, A. H., and Lieberman, G. J., 1959, *Engineering Statistics*, Prentice-Hall, Englewood Cliffs, NJ.
[43] Dipasquale, E., Ju, J., Askar, A., and Cakmak, A., 1990, "Relation Between Global Damage Indices and Local Stiffness Degradation," J. Struct. Eng., **116**(5) [May.], pp. 1440–1456.
[44] Myklestad, N. O., 1944, "A New Method of Calculating Natural Modes of Uncoupled Bending Vibration of Airplane Wings and Other Types of Beams," J. Aeronaut. Sci., **12**, pp. 153–162.
[45] Thomson, W. T., 1972, *Theory of Vibrations with Applications*, Prentice-Hall, Englewood Cliffs, NJ.
[46] Pestel, E. C., and Leckie, F. A., 1963, *Matrix Methods in Elastomechanics*, McGraw-Hill, New York.
[47] Meirovitch, L., 2001, *Fundamentals of Vibrations*, McGraw Hill, New York.
[48] Myklestad, N., 1944, *Vibration Analysis*, McGraw-Hill, New York.